Published by

World Scientific Publishing Co. Pte. Ltd.
P O Box 128, Farrer Road, Singapore 912805
USA office: Suite 1B, 1060 Main Street, River Edge, NJ 07661
UK office: 57 Shelton Street, Covent Garden, London WC2H 9HE

British Library Cataloguing-in-Publication Data
A catalogue record for this book is available from the British Library.

ISBN 981-02-4315-4

Printed in Singapore by Uto-Print

Peyresq Lectures on

Nonlinear Phenomena

Editors

Robin Kaiser
James Montaldi

Institut Non Linéaire de Nice, France

World Scientific
Singapore • New Jersey • London • Hong Kong

MATHEMATICAL MODELLING IN THE LIFE SCIENCES: APPLICATIONS IN PATTERN FORMATION AND WOUND HEALING

PHILIP K. MAINI
Centre for Mathematical Biology, Oxford

1 Introduction

Spatial and spatio-temporal patterns occur widely in the life sciences as well as in chemistry. Perhaps the best-known example of spatio-temporal pattern formation is the spontaneous generation of propagating fronts, target patterns, spiral waves and toroidal scrolls in the Belousov-Zhabotinsky reaction, in which bromate ions oxidise malonic acid in a reaction catalysed by cerium, which has the states Ce^{3+} and Ce^{4+}. Sustained periodic oscillations are observed in the cerium ions. If, instead, one uses the catalyst Fe^{2+} and Fe^{3+} and phenanthroline, the periodic oscillations are visualised as colour changes between reddish-orange and blue (see, for example, Murray, 1993, Johnson and Scott, 1996 for review). Similar types of patterning arise in physiology and one of the most widely-studied and important areas of wave propagation concerns the electrical activity in the heart (Panfilov and Holden, 1997) which stimulates muscle contraction resulting in the heart beating.

Understanding the mechanisms underlying spatio-temporal pattern formation is a central goal in embryology. Although genes control pattern formation, genetics does not give us an understanding of the actual mechanisms involved in patterning. Many models of how different processes can conspire to produce pattern have been proposed and analysed. They range from gradient-type models involving a simple source-sink mechanism (Wolpert, 1969); to cellular automata models in which the tissue is discretised and rules are introduced as to how different elements interact with each other (see, for example, Bard, 1981); to more complicated models which incorporate more sophisticated chemistry, physics and biology, and which propose that patterns are set up due to self-organisation rather than as a consequence of externally imposed cues. All of these models focus on the key question of how cells respond to and interact with signalling cues. This is a crucial question in a number of areas of the biomedical sciences. For example, in tumour formation, one wishes to understand how the signalling cues involved in the regulation of cellular processes no longer function properly. Many of the physical processes that occur

during the formation and spread of tumour cells are also of vital importance in wound healing, where their function benefits the organism rather than being destructive to it. Recent advances in molecular and cellular biology have led to the rapid development of experimental research into the biochemical mechanisms underlying the processes of wound healing. Wound healing is an enormously complex dynamic spatio-temporal process and new insights are being gained by focussing on the interaction of specific processes involved for a particular aspect of healing.

In all the above areas, a number of complex mechanical and biochemical processes are interacting in a highly nonlinear way. Such systems are amenable to mathematical modelling and the role of the modeller is to suggest explanations, based on biologically plausible mechanisms, of observed behaviour and to make experimentally testable predictions.

In this article, I will review, in Section 2, some of the commonly used models for pattern formation in early development. In Section 3 I will describe some models that have been used to address particular phenomena in wound healing. At the end of each section, a discussion on the particular applications is presented. Section 4 contains a general discussion and points to future directions.

2 Models for pattern formation and morphogenesis

Cell fate and position within the embryo can be strongly influenced by environmental factors. Therefore, to answer questions on pattern formation, one must really address the issue of how the embryo organises the complex spatio-temporal sequence of signalling cues necessary to develop structure in a controlled and coordinated manner. Structure can form through tissue movement and rearrangement, cell-cell interaction, or in response to chemical signals. We first consider the latter type of model.

2.1 Chemical pre-pattern models

The simplest chemical pre-pattern model is the gradient model proposed by Wolpert (1969) in which a source-sink mechanism, coupled with diffusion and degradation, leads to a spatial gradient in a single morphogen. He proposed that this provided *positional information* for cells, which differentiated according to a series of threshold values. More complicated spatial patterns can be generated due to the reaction and diffusion of a number of chemicals. This phenomenon is known as *diffusion-driven instability* and was first proposed by Turing in a seminal paper (Turing, 1952). The reaction kinetics he considered were stabilizing and diffusion is, of course, a homogenizing process. Yet combined in the appropriate way, these two stabilizing influences can conspire to produce an instability which can result in spatially heterogeneous chemical profiles – a spatial pattern. This is an example of an *emergent property* and is termed *diffusion-driven instability*, that is, a spatially uniform steady state, linearly stable in the absence of diffusion, becomes linearly unstable in the presence of diffusion.

To derive the partial differential equation form of Turing's model, let us first consider a single chemical, with concentration $c(\mathbf{x}, t)$ at position $\mathbf{x} \in \mathbf{R}^3$ and time $t \in [0, \infty)$. Consider an arbitrary volume $V \subset \mathbf{R}^3$. Then
rate of change of chemical in V = – flux + net production i.e.

$$\frac{d}{dt}\int_V c dv = -\int_{\partial V} \mathbf{F}.d\mathbf{S} + \int_V f(c)dv \tag{1}$$

where $\mathbf{F}$ is the flux of chemical per unit area and $f(c)$ is net chemical production per unit volume. On using the divergence theorem and the fact that the volume V is arbitrary, this equation becomes

$$\frac{\partial c}{\partial t} = -\nabla.\mathbf{F} + f(c). \tag{2}$$

The function $\mathbf{F}$ is determined by Fick's Law, which states that chemical flux is proportional to the concentration gradient, i.e.

$$\mathbf{F} = -D\nabla c \tag{3}$$

where D is the diffusion coefficient. Therefore the reaction-diffusion equation governing the spatio-temporal evolution of c takes the form:

$$\frac{\partial c}{\partial t} = \nabla.(D\nabla c) + f(c). \tag{4}$$

To complete the model formulation we need to specify initial conditions, $c(\mathbf{x}, 0) = c_0(\mathbf{x})$ and boundary conditions. The latter may typically be periodic, zero flux or fixed, depending on the phenomenon being modelled.

The above derivation can be generalised easily to a system of interacting chemicals leading (in the case of constant diffusion coefficients) to

$$\frac{\partial \mathbf{u}}{\partial t} = \mathbf{D}\nabla^2\mathbf{u} + \mathbf{f}(\mathbf{u}), \tag{5}$$

where $\mathbf{u}$ is a vector of chemical concentrations, $\mathbf{u} = (u_1, u_2, ..., u_n)^T$; $\mathbf{f} = (f_1(\mathbf{u}), f_2(\mathbf{u}), ..., f_n(\mathbf{u}))^T$ and models chemical interaction; and $\mathbf{D}$ is an $n \times n$ diffusion matrix. In the simplest examples, $\mathbf{D}$ is a diagonal matrix. More generally, $\mathbf{D}$ can have off-diagonal terms to model cross-diffusion.

The classical reaction-diffusion model is a system of two chemicals, u and v, reacting and diffusing as follows:

$$\frac{\partial u}{\partial t} = D_1 \nabla^2 u + f(u,v) \tag{6}$$

$$\frac{\partial v}{\partial t} = D_2 \nabla^2 v + g(u,v). \tag{7}$$

We will assume zero flux boundary conditions. The functions f and g are rational functions of u and v (see examples later). Using standard linear analysis (see, for example, Murray, 1993) it can be shown that a spatially uniform steady state of the above system can undergo diffusion-driven instability if the following conditions hold:

(C.1) $f_u + g_v < 0$

(C.2) $f_u g_v - f_v g_u > 0$

(C.3) $D_1 g_v + D_2 f_u > 2\sqrt{D_1 D_2 (f_u g_v - f_v g_u)}$

where all the partial derivatives are evaluated at the spatially uniform steady state.

One possible scenario for pattern formation is that in which f_u and g_u are positive, the latter implying that u *activates* v, while g_v and f_v are negative, so that v *inhibits* u (see, for example, Dillon *et al.*, 1994). Condition (C.1) $\Rightarrow |f_u| < |g_v|$, so from (C.3) $D_1 < D_2$. That is, the activator diffuses more slowly than the inhibitor. This is an example of the classic property of many self-organising systems, namely *short-range activation, long-range inhibition.*

In Turing's original model, f and g were linear so that, if the uniform steady state became unstable, then the chemical concentrations would grow exponentially. This, of course, is biologically unrealistic. Since Turing's paper, a number of models have been proposed wherein f and g are nonlinear so that when the uniform steady state becomes unstable, it may or may not evolve to a bounded, stationary, spatially non-uniform, steady state (a *spatial pattern*) depending on the nonlinear terms.

These models may be classified into four types:

(i) Phenomenological Models: The functions f and g are chosen so that one of the chemicals is an activator, the other an inhibitor. An example is the Gierer-Meinhardt model (1972), for which

$$f(u,v) = \alpha - \beta u + \frac{\gamma u^2}{v}, \quad g(u,v) = \delta u^2 - \eta v \tag{8}$$

where $\alpha, \beta, \gamma, \delta$ and η are positive constants, u activates v and v inhibits u.

(ii) Hypothetical Models: Derived from a hypothetically proposed series of chemical reactions. For example, Schnakenberg (1979) proposed a series of trimolecular autocatalytic reactions involving two chemicals as follows

$$X \underset{k_2}{\overset{k_1}{\rightleftharpoons}} A, \quad B \xrightarrow{k_3} Y, \quad 2X + Y \xrightarrow{k_4} 3X.$$

Using the Law of Mass Action, which states that the rate of reaction is directly proportional to the product of the active concentrations of the reactants, and denoting the concentrations of X, Y, A and B by u, v, a and b, respectively, we have

$$f(u,v) = k_2 a - k_1 u + k_4 u^2 v, \quad g(u,v) = k_3 b - k_4 u^2 v \tag{9}$$

where $k_1, ..., k_4$ are (positive) rate constants. Assuming that there is an abundance of A and B, a and b can be considered to be approximately constant.

(iii) Empirical Models: The kinetics are fitted to experimental data. For example, the Thomas (1975) immobilized-enzyme substrate-inhibition mechanism involves the reaction of uric acid (concentration u) with oxygen (concentration v). Both reactants diffuse from a reservoir maintained at constant concentration u_0 and v_0, respectively, onto a membrane containing the immobilized enzyme uricase. They react in the presence of the enzyme with empirical rate $\frac{V_m uv}{K_m + u + u^2/K_s}$, so that

$$\begin{aligned} f(u,v) &= \alpha(u_0 - u) - \frac{V_m uv}{K_m + u + u^2/K_s}, \\ g(u,v) &= \beta(v_0 - v) - \frac{V_m uv}{K_m + u + u^2/K_s} \end{aligned} \tag{10}$$

where α, β, V_m, K_m and K_s are positive constants.

(iv) Actual Chemical Reactions: Although Turing predicted, in 1952, the spatial patterning potential of chemical reactions, this phenomenon has only recently been realised in actual chemical reactions. Therefore, it is now possible in certain cases to write down detailed reaction schemes and derive, using the Law of Mass Action, the kinetic terms.

The first Turing patterns were observed in the chlorite-iodide-malonic acid starch reaction (CIMA reaction) (Castets *et al.*, 1990, De Kepper *et al.*, 1991). The model proposed for this reaction by Lengyel and Epstein (1991) stresses three processes: the reaction between malonic acid (MA) and iodine to create iodide, and the reactions between chlorite and iodide and chloride and iodide. These reactions take the form

$$MA + I_2 \rightarrow IMA + I^- + H^+$$

$$ClO_2 + I^- \rightarrow ClO_2^- + \frac{1}{2}I_2$$

$$ClO_2^- + 4I^- + 4H^+ \rightarrow Cl^- + 2I_2 + 2H_2O.$$

The rates of these reactions can be determined experimentally. By making the experimentally realistic assumption that the concentration of malonic acid, chlorine dioxide and iodine are constant, Lengyel and Epstein derived the following model:

$$\frac{\partial u}{\partial t} = k_1 - u - \frac{4uv}{1+u^2} + \nabla^2 u$$

$$\frac{\partial v}{\partial t} = k_2\left[k_3\left(u - \frac{uv}{1+u^2}\right) + c\nabla^2 v\right]$$

where u, v are the concentrations of iodide and chlorite, respectively and k_1, k_2, k_3 and c are positive constants.

Murray (1982) calculates and compares the parameter spaces determined by (C.1)-(C.3) for linear instability in the Gierer-Meinhardt, Schnakenberg and Thomas models.

In many cases, particularly in one dimension, the results of the linear analysis carry over to the weakly nonlinear case but the fully nonlinear system can only be analysed by numerical simulation. There is now a great deal of literature on this subject and general results on the patterning properties of reaction-diffusion equations can be found in the books by Britton (1986), Edelstein-Keshet (1988), Fife (1979), Grindrod (1996), Murray (1993) and Segel (1984).

The gradient models and the Turing-type models differ in two crucial aspects: In the gradient model, the chemical pre-pattern is set up by a simple process which can only produce a simple gradient. To use this gradient to generate complicated pattern, it is hypothesized that a complex series of thresholds exist and cells have the machinery to interpret multiple thresholds. In Turing's model, complex spatial patterns arise due to a complex chemical interaction, but the interpretation of the pre-pattern is via a single threshold (Nagorcka, 1989) and is therefore simpler than that in the gradient model.

2.2 *Cell movement models*

Cell movement models are based on the assumption that a spatial pattern arises in cell density, and cells then differentiate in a density-dependent manner. Cell aggregation occurs when the cell dispersing factors (for example, diffusion) are overcome by aggregating factors such as chemotaxis (movement up chemical gradients), or factors generated by the mechanical interaction of cells with the extracellular matrix (ECM) on which they move. These include haptotaxis (movement up adhesive gradients) or passive convection arising as the result of deformation of the ECM due to cell traction. Chemotactic models have been analysed by a number of authors and shown to lead to spatial pattern formation (see, for example, Keller and Segel, 1971; Maini *et al.*, 1991). These models involve reaction and diffusion, but spatial patterning arises in this case due to the advective term introduced by chemotaxis. The typical model takes the form:

$$\frac{\partial n}{\partial t} = D_n\nabla^2 n - \nabla.(\chi(u)n\nabla u) + f(n,u) \tag{11}$$

$$\frac{\partial u}{\partial t} = D_u\nabla^2 u + g(n,u), \tag{12}$$

where $n(\mathbf{x},t), u(\mathbf{x},t)$ denote cell density and chemoattractant concentration, respectively, at position $\mathbf{x}$ and time t; D_n, D_u are diffusion coefficients, f, g are terms incorporating production and degradation and $\chi(u)$ is the chemotactic sensitivity. The latter varies depending on the mode of cell-chemoattractant interaction (Othmer and Stevens, 1997).

The first partial differential equation model incorporating the role of mechanical cues in the formation of cell aggregation was proposed by Oster *et al.* (1983) and since then such models have been extensively studied (Murray, 1993). They consist of conservation equations for cells and extracellular matrix, which take the general form of the equations above, but the main difference is the force-balance equation, which is that for a viscoelastic material. The mechanical model proposed by Oster *et al.* (1983) has three dependent variables: $n(\mathbf{x},t)$, $\rho(\mathbf{x},t)$ and $\mathbf{u}(\mathbf{x},t)$ which represent, respectively, cell density, matrix density and matrix displacement at position $\mathbf{x}$ and time t.

The cell equation is

$$\frac{\partial n}{\partial t} = -\nabla.\mathbf{J} + rn(N-n) \tag{13}$$

where net cell production is assumed to be of logistic form, r and N are positive constants, and $\mathbf{J}$, the cell flux, is given by $\mathbf{J} = -D\nabla n + \alpha n\nabla\rho + n\frac{\partial \mathbf{u}}{\partial t}$.

The first term on the right-hand side models random motion and the third term accounts for passive advection. Cells can also move by attaching cell processes to adhesive sites within the matrix and crawling along. As cells exert forces on the extracellular matrix they generate adhesive gradients which serve as guidance cues to motion. The movement up such gradients is termed haptotaxis. The assumption that the number of adhesive sites is proportional to ECM density leads to the second term on the right-hand side, where α is the haptotactic coefficient, assumed to be a non-negative constant. Hence the equation for cell motion is

$$\frac{\partial n}{\partial t} = D\nabla^2 n - \alpha\nabla.(n\nabla\rho) - \nabla.\left(n\frac{\partial \mathbf{u}}{\partial t}\right) + rn(N-n). \tag{14}$$

The equation for ECM density is much simpler as the only contribution to matrix flux is advection, and matrix secretion is assumed negligible. Hence, ρ satisfies

$$\frac{\partial \rho}{\partial t} = -\nabla.\left(\rho\frac{\partial \mathbf{u}}{\partial t}\right). \tag{15}$$

To derive the equation for the matrix displacement, $\mathbf{u}(\mathbf{x}, t)$, we first note that for cellular and embryonic processes, inertial terms are negligible in comparison to viscous and elastic forces, that is, motion ceases instantly when the applied forces are turned off. Hence the traction forces generated by the cells are balanced by the viscoelastic forces within the ECM. Therefore the equilibrium equations are

$$\nabla.\sigma + \rho\mathbf{F} = \mathbf{0} \tag{16}$$

where σ is the composite stress tensor of the cell-ECM milieu and $\rho\mathbf{F}$ accounts for body forces.

Oster *et al.* (1983) model the cell-matrix composite as a linear viscoelastic material with stress tensor

$$\sigma = \sigma_\rho + \sigma_n. \tag{17}$$

Here σ_ρ is the usual viscoelastic stress tensor (see, for example, Landau and Lifshitz, 1970),

$$\sigma_\rho = \underbrace{\mu_1\frac{\partial \varepsilon}{\partial t} + \mu_2\frac{\partial \theta}{\partial t}\mathbf{I}}_{\text{viscous}} + \underbrace{\frac{E}{1+\nu}\left(\varepsilon + \frac{\nu}{1-2\nu}\theta\mathbf{I}\right)}_{\text{elastic}} \tag{18}$$

where: $\theta = \nabla.\mathbf{u}$ is the dilatation, $\varepsilon = \frac{1}{2}[\nabla\mathbf{u} + \nabla\mathbf{u}^T]$ is the stress tensor, $\mathbf{I}$ is the unit tensor, μ_1, μ_2 are the shear and bulk viscosities, respectively, and E, ν are the Young's modulus and the Poisson ratio, respectively.

The stress due to cell traction is modelled by

$$\sigma_n = \frac{\tau n\rho}{1+\lambda n}\mathbf{I} \tag{19}$$

where τ and λ are positive constants. This satisfies the conditions that there is no traction without matrix and that traction per cell decreases with increasing cell density (contact inhibition).

If the cell-matrix composite is attached to an external substratum, for example a subdermal basement layer, then the simplest way to model the body force is to assume

$$\mathbf{F} = s\mathbf{u} \tag{20}$$

where s is the modulus of elasticity of the substrate to which the composite is attached.

With appropriate boundary conditions (for example zero flux on n and ρ, with $\mathbf{u}$ fixed) the above equations for cell density, matrix density and displacement define a simple version of the more complicated mechanical model presented by Oster *et al.* (1983).

Linear and nonlinear analyses, plus numerical simulation, show that models within this general mechanical framework can exhibit steady-state spatial patterns (Perelson *et al.*, 1986) and spatio-temporal patterns (Ngwa and Maini, 1995).

Other movement models hypothesize that cells move to minimize energy (Cocho *et al.*, 1987a,b; Steinberg, 1970; Sulsky, 1984). Such models can be set up mathematically and solved to show cell sorting and patterning behaviour consistent with a number of experimentally observed phenomena.

2.3 Cell rearrangement models

Theoretical studies in this area include the early purse-string model of Odell *et al.* (1981) for tissue folding in which, in response to a large deformation, cells were proposed to actively contract and in so doing cause a large deformation in neighbouring cells which, in turn, also contract, setting up a propagating contraction wave which leads to tissue folding. This model was applied to a variety of developmental problems, and provided the precursor to the "mechanochemical theory" of developmental pattern formation reviewed above. This approach emphasises the link between tissue mechanics and chemical regulation, and has been applied widely in both developmental biology and medicine. Subsequently, Weliky and Oster developed a discrete-cell modelling approach in which morphogenesis occurs via mechanical rearrangement

of neighbours in an epithelial sheet. They assume that the boundary of the epithelial sheet is pulled over the surface of the egg and show that the resultant model can produce many experimentally observed aspects of both *Fundulus* epiboly and notochord morphogenesis in *Xenopus laevis* (Weliky and Oster, 1990; Weliky *et al.*, 1991). More recently, Davidson *et al.* (1995) used a computational finite element model to test various explanations for sea urchin invagination.

In all these models individual cell movements within the tissue are determined by the balance of mechanical forces acting on the cell. Such models can exhibit tissue folding, thickening, invagination, exogastrulation and intercalation, and have been shown to capture many of the key aspects of processes such as gastrulation, neural tube formation, and ventral furrow formation in *Drosophila*. Models for tissue motion are not amenable to a mathematical analysis and tend to be highly computation-based.

2.4 Applications

Turing considered the chemicals in his model to be growth hormones, so that the spatial pattern in chemical concentrations would result in spatially non-uniform growth and hence pattern. He applied his theory to account for budding in plant stems and to growth-induced shape changes in the early embryo which he proposed could account for gastrulation. Since his seminal paper, reaction-diffusion models have been proposed to account for a vast number of patterning processes in nature, too great to be completely reviewed here, so we consider only a few examples to give a flavour of the applications.

Gierer and Meinhardt (1972) used their model to account for pattern formation in *Hydra* and showed that this model could account for the remarkable regenerative properties exhibited by this organism. Reaction-diffusion models have been proposed to account for compartmentalisation in insect development and to provide an explanation for the occurrence of various mutants (see Meinhardt, 1982, for review). However, for *Drosophila* it now appears that patterning is due to a cascade of protein interactions that are consistent with the gradient-type models and are not of Turing-type.

Meinhardt (1995) has shown that reaction-diffusion type models solved on a growing domain can produce the spectacular variety of patterns seen on shells (Figure 1), while Nijhout (1990) has shown that such models, together with a small number of sources and sinks, can exhibit the vast array of pigmentation patterns observed on butterfly wings. Shell patterns can also be produced by an integro-partial differential equation model aimed at capturing neural activity along the front of the growing shell (Ermentrout *et al.*, 1986).

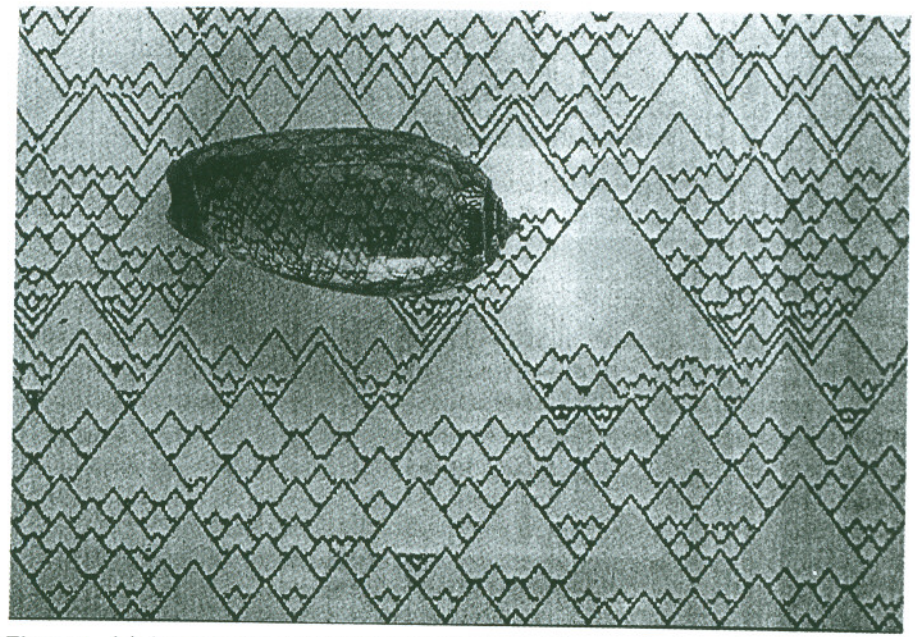

Figure 1. (a) Spatial pattern exhibited on the shell *Oliva porphyria* and a simulation of a reaction-diffusion model on a large array of cells. (Reproduced with permission from Meinhardt, 1995).

Although this model is based on very different biology to the reaction-diffusion model and has a different mathematical form, it still falls under the general category of short-range activation, long-range inhibition models.

Reaction-diffusion and cell movement models have been applied to animal coat markings (Bard, 1981; Cocho *et al.*, 1987a,b; Murray, 1981; Murray and Myerscough, 1991) and to skeletal patterning in the limb, for which gradient models have also been proposed (see Maini and Solursh, 1991, for a critical review).

The above models propose different scenarios for pattern formation and, to date, it is a highly controversial issue as to which model is the appropriate one. Chemical morphogens, the name given to the chemicals proposed to form pre-patterns, have yet to be unequivocally identified, so it is difficult

to fix parameter values. For the mechanical type model mentioned above, parameters are also difficult to determine. Moreover, the original model is based on the Kelvin model of linear viscoelasticity and there is no justification for taking this particular form. The Maxwell model will also give rise to pattern formation, but for different parameter values (Byrne and Chaplain, 1996). Thus, without constraints on the parameter values, one can produce similar patterns with each model and therefore cannot distinguish between them on that basis.

It is also difficult to distinguish, from a biological viewpoint, between models. For example, in some cases one observes both a chemical pattern and a cell aggregation pattern but it is difficult biologically to determine which came first. The chemical pre-pattern model would say that the chemical pattern arose first and cells responded to this by differentiating, resulting in cell condensations. The cell-chemotaxis model scenario would be that both patterns arise simultaneously, while under the assumptions in the mechanical model, the patterns would be explained by cell aggregations first forming and then secreting a chemical pattern as a result of differentiation.

Although these models are based on very different biological assumptions, many of them share common properties. For example, the patterning in reaction-diffusion and in many cell movement models arises from the interaction of the processes of *short-range activation, long-range inhibition.* On the one hand, this has the disadvantage of making it very difficult to use models to distinguish between mechanisms, on the other hand, it does mean that one can make general conclusions and predictions that are *mechanism-independent.* This leads to the idea of *developmental constraints* which proposes that only certain patterns are possible, regardless of the mechanism (Oster and Murray, 1989). Figure 2 illustrates one such developmental constraint.

A key property of many development processes is their robustness in the face of naturally occurring random fluctuations. This has been a major problem for reaction-diffusion theory, as it is well-known that the patterns it produces are not robust (Bard and Lauder, 1974). In other words, Turing-type models can exhibit multiple stable solutions in large regions of parameter space. Recently it has been shown that boundary conditions can play a crucial role in stabilizing patterns. For example, if one chooses fixed boundary conditions for one chemical and zero flux boundary conditions for the other, then this reduces the number of admissible solutions and thus diminishes the regions in parameter space in which one obtains multiple stable solutions. In effect, the boundary conditions serve to select only certain patterns (Dillon *et al.*, 1994).

In higher dimensions, this problem becomes more acute as one now has

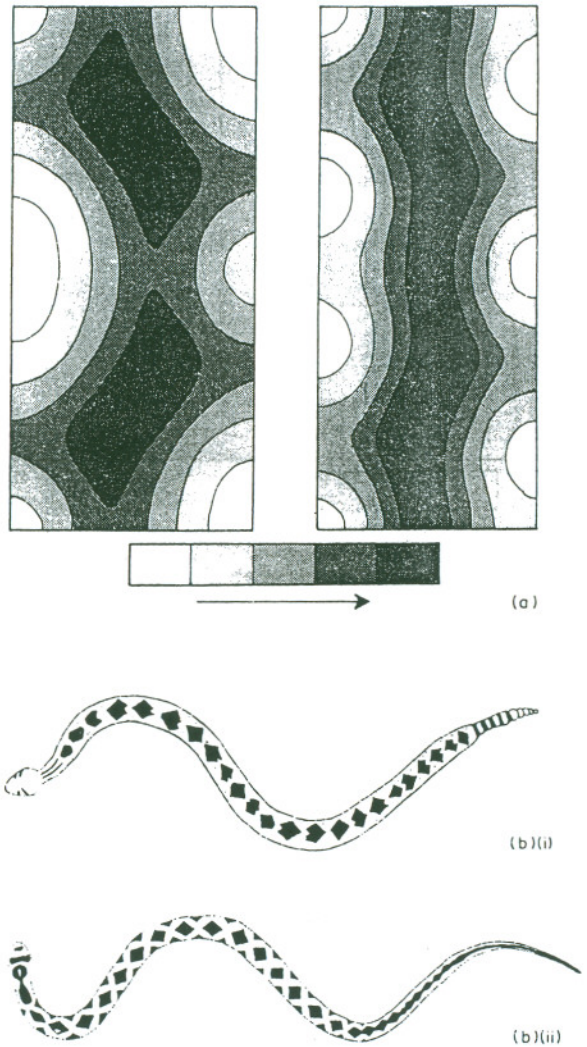

Figure 2. Simulation of a cell-chemotaxis model of the form (11) – (12) showing the effect of domain size on cell density concentration (arrow denotes increasing cell density). As the domain narrows, the diamond pattern changes to a simpler, wavy stripe pattern. This is an example of a developmental constraint. (b) Examples of diamond patterns on snakes (i) *Crotalus adamanteus*; (ii) *Coluber hippocrepis* (note the effect of the tapering domain). Reproduced with permission from Murray and Myerscough, 1991.

the added problem of degeneracy. For example, for certain parameters, there may be two or more admissible solutions with the same linear growth rate and it is then not clear which solution is selected. Using nonlinear bifurcation analysis, Ermentrout (1991) showed that the nonlinear terms play a key role in pattern selection, with quadratic terms favouring spots, while cubic terms favour stripes. More recently, Benson *et al.* (1998) have shown how a spatially-varying parameter can unravel such degeneracies and select one pattern over another. The role of spatially-varying parameters has received little attention (although it should be noted that the Gierer-Meinhardt model was initially designed to explain how localized structures could arise in places determined by a pre-existing gradient) but they can play a crucial role in the patterning process. For example, Wolpert and Hornbruch (1990) showed experimentally that double-anterior chick limb buds gave rise to two humeri, even though the size of the bud was the same as that of a normal limb bud, which only produces one humerus. This contradicts the standard Turing model, which predicts that patterning complexity is intimately linked to domain size. Maini *et al.* 1992, showed that a Turing model with spatially-varying diffusion coefficients could give rise to results that are consistent with Wolpert and Hornbruch's experiments. Results of dye-spreading experiments suggest that the hypothesis of spatially-varying diffusion is very plausible (Brümmer *et al.*, 1991).

These studies have all been carried out on the reaction-diffusion model system because it is the simplest, mathematically speaking, of the models reviewed in this section. It is still an open question as to whether the results on robustness, pattern selection and spatially-varying parameters carry through to the other model types.

In all the above applications, patterns occur simultaneously throughout the whole domain. However, in some cases, patterns arise as the result of propagation. For example, in the alligator embryo, the pigmentation stripes occur as a propagating pattern moving down the body from head to tail. Murray *et al.* (1990), have shown that a cell-chemotactic model of the form discussed above can give rise to such patterns. They were able to make experimentally confirmed predictions on how the number of stripes varies with the length of the embryo and present biological evidence that supports the view that this is a cell movement process.

More recently, Painter *et al.* (1999a) have studied the formation of the primitive streak. This is a novel patterning process wherein, during the blastoderm stage of early chick development, a column of cells, known as the primitive streak, advances to about 3/5 the way across the disk-shaped blastoderm, before regressing. They have shown how this could arise from a

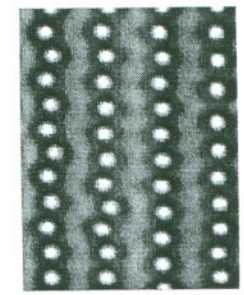

Thirteen–lined Ground Squirrel

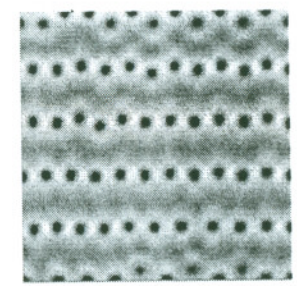

Pomacanthus maculatus

Figure 3. Coupling two reaction-diffusion models can lead to a complicated pattern of stripes interspersed with spots, as observed in the thirteen-lined ground squirrel and *Pomacanthus maculatus*. (Reproduced with permission from Aragón *et al.*, 1998).

cell-chemotaxis type model and have made a number of testable predictions.

2.5 Coupling pattern generators

In many cases, pattern formation arises as the result of the interaction of more than one pattern generator. For example, epidermal-dermal interactions play a crucial role in the development of skin organs, such as hair, teeth, feathers and scales. Nagorcka *et al.* (1987) considered a tissue-tissue interaction model that coupled a mechanochemical cell movement model in the dermis with a

reaction-diffusion model in the epidermis. They showed that such a model can give rise to patterns on two different length scales, namely, large spots interspersed with small spots, and these are similar to the scale patterns observed in certain lizards and to the feather germ patterns observed on certain birds. More recently, Aragón *et al.* (1998) have shown how the coupling between two systems of reaction-diffusion models can produce complex patterns (see Figure 3).

The life cycle of the cellular slime mould *Dictyostelium discoideum* serves as an excellent paradigm for morphogenesis as it exhibits the processes of signal transduction, signal relay, cell movement and aggregation, all of which play important roles in early embryonic development. Hence, for many years, it has attracted the interest of developmental biologists and theoreticians alike. Starvation conditions trigger a developmental programme which is initiated by cell-cell signalling via the extracellular messenger cyclic 3'5'-adenosine monophosphate (cAMP). The chemotactic response to this signal leads, through the phenomenon of cell streaming, to the formation of a multicellular organism composed typically of $10^4 - 10^5$ cells. This organism passes through an intermediate motile (slug) phase during which cells differentiate into pre-spore and pre-stalk types, before developing a fruiting body, aiding the dispersal of spores from which, under favourable conditions, new amoebae develop. The comparative simplicity of morphogenesis in *Dictyostelium* has made it an attractive model system for the study of self-organisation, and many of the molecular and cellular mechanisms which are involved in cell aggregation, collective movement and differentiation have now been identified.

Several models have been proposed to account for many of the aforementioned phenomena. Here, we shall focus on a model for cell aggregation proposed by Höfer *et al.* (1995a,b) – we refer the reader to this paper for a fuller description of the biology and parameter values, as well as references to other models. The model takes the form:

$$\frac{\partial n}{\partial t} = \nabla \cdot (\mu \nabla n - \chi(v) n \nabla u) \tag{21}$$

$$\frac{\partial u}{\partial t} = \lambda[\phi(n) f_1(u,v) - (\phi(n) + \delta) f_2(u)] + \nabla^2 u \tag{22}$$

$$\frac{\partial v}{\partial t} = -g_1(u)v + g_2(u)(1-v), \tag{23}$$

where n, u and v denote cell density, extracellular cAMP concentration and fraction of active cAMP receptors, respectively.

The second and third equations are a simplified model of the cAMP-cell receptor dynamics (see Martiel and Goldbeter, 1987, for full details) modified by cell density effects; the rate of cAMP synthesis per cell is $f_1(u,v) = (bv + v^2)(a + u^2)/(1 + u^2)$, where a and b are positive constants. This models autocatalytic production with saturation, mediated by receptor binding. The functions f_2 and g_1 are assumed to be linear in u, to model linear degradation of cAMP and binding of active receptors to cAMP, respectively, while g_2 is assumed to be a positive constant, accounting for the resensitization of the desensitized fraction of receptors at constant rate. This subsystem exhibits excitable dynamics leading to the formation of spiral waves of cAMP concentration. Cell density effects are modelled by the factor $\phi(n) = n/(1-\rho n/(K+n))$, where ρ and K are positive constants. This excitable system is coupled with a chemotaxis equation for cell density, with constant diffusion coefficient μ, and chemotactic sensitivity $\chi(v) = \chi_0 v^m/(A^m + v^m)$, $m > 1$, which accounts for adaptation, where χ_0 and A are positive constants. Hence an appreciable chemotactic response requires a minimal fraction of active receptors, yet, for a large fraction of active receptors, the response saturates. Note that many models of chemotaxis assume χ to be a constant. Under that assumption, cells would respond to a pulse of chemoattractant by moving towards the wave in the wavefront, then moving with the wave in the waveback, resulting in a net movement away from the source of attractant, rather than towards it. This is the so-called "chemotactic wave paradox" (Soll *et al.*, 1993). The form of $\chi(v)$ chosen above resolves this paradox (Höfer *et al.*, 1994).

Using experimentally determined parameter values, the above model captures the key features of the aggregation process (see Figure 4). The model is consistent with the observation that as streaming proceeds, the wavespeed and wavelength of the spiral patterns decrease (Gross *et al.*, 1976). Previously, this has been explained by assuming that biochemical changes must be occurring in the cell-cAMP system and, indeed, it has now been established that changes of this sort can occur. However, in the above model, this behaviour arises naturally, because as the cells form streams, they alter the conditions through which the cAMP waves are propagating. This is initially equivalent to increasing the excitability of the medium which, in turn, leads to an increase in the rotation frequency of the spiral core. As a result (Tyson and Keener, 1988) the wavespeed and wavelength of the spiral patterns decrease.

2.6 *Domain Growth*

None of the above models account for domain growth. However, a number of recent studies have shown that domain growth can play a vital part in the pattern formation process. For example, Kondo and Asai (1995) showed that the pigmentation pattern in the juvenile angelfish *Pomacanthus semicirculatis*, exhibits changes in the number of stripes as it grows. Briefly, when the wave-

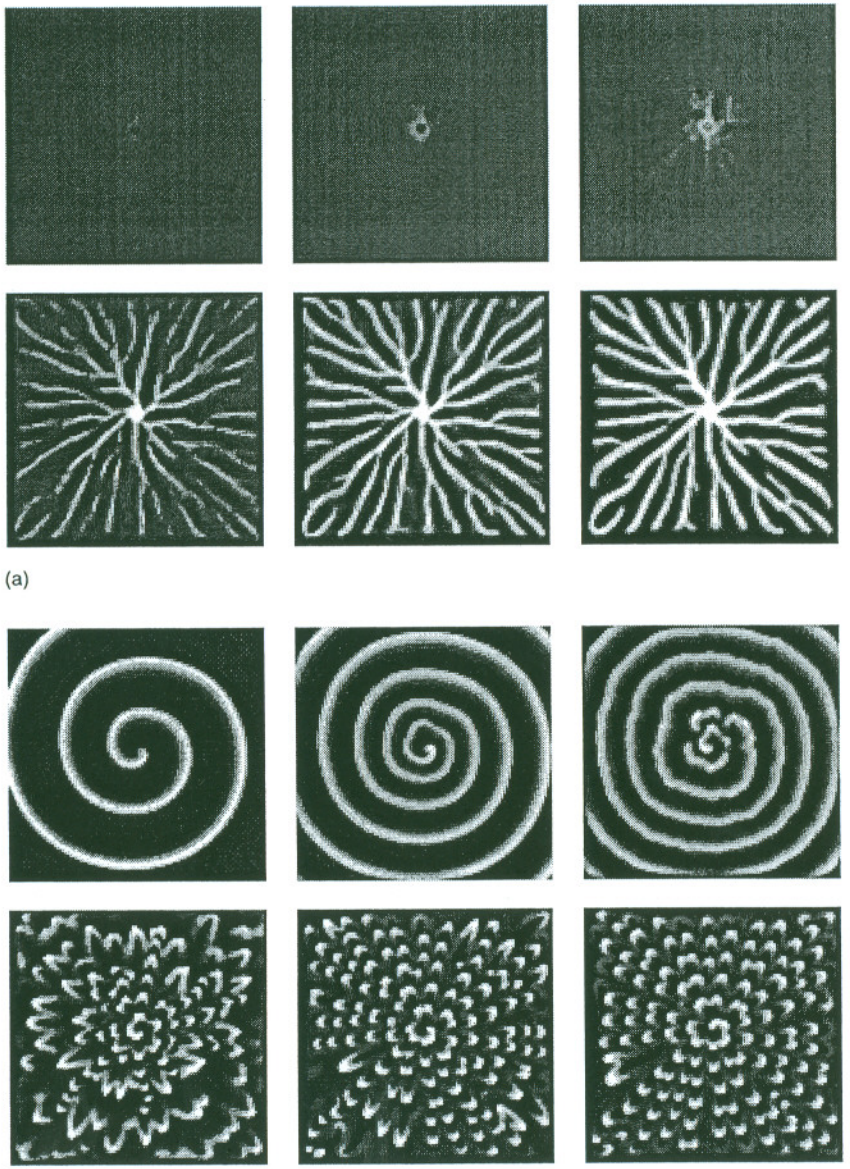

Figure 4. Spatio-temporal evolution of (a) cell density, and (b) cAMP concentration in a numerical simulation of (21)–(23). (Reproduced with permission from Höfer *et al.*, 1995b).

length of the stripes increases twofold due to domain growth, further stripes are inserted to restore the wavelength to its original value. They showed that this is consistent with a reaction-diffusion model. More recently, Painter *et al.* (1999b) showed that a cell-chemotaxis model coupled with a reaction-diffusion model on a growing domain could account also for the fact that the inserted stripes are thinner than the original stripes. This phenomenon is not easily explained by a reaction-diffusion model.

It is believed that domain growth also plays a role in the determination of the sites of tooth primordia in alligators. The first seven tooth primordia of the lower alligator jaw occur (taking one half of the jaw) in the spatio-temporal sequence 4-1-5-2-6-3-7, that is, the fourth primordia to form is the posterior-most while the seventh primordia to form is the anterior-most. Kulesa *et al.* (1996) have shown how a reaction-diffusion model coupled with an inhibitor model on a growing domain could explain this sequence.

More recently, Crampin *et al.* (1999) have shown that domain growth can lead to the robust pattern selection of certain types of patterns in reaction-diffusion models, while Holloway and Harrison (1999) have shown that inter-specific variation in branching patterns in certain plants can be accounted for by a system of reaction-diffusion equations on a growing two-dimensional domain in which growth is controlled by the concentration of one of the chemicals.

2.7 *Discussion*

Development of spatial pattern and form is unquestionably one of the central areas in biology. It is a very complex process that involves the interaction of a large number of components acting at different levels, yet the models presented in this section focus on only a small number of components. An important question to ask therefore, is that although it is clear that even these simple models offer theoreticians an enormous range of challenging problems from modelling, numerical computation and mathematical viewpoints, what does it actually say about the biology? The models presented here are really of two types. The first are conceptual, for example, it is remarkable that the simple mechanism of short-range activation, long-range inhibition can give rise to such an enormous range of patterns. One can think of this as being a primary mechanism for generating spatial pattern. Such models provide a framework in which one can test theories of patterning, as well as making experimentally testable predictions.

The second type of model is where more is known about the biochemistry and parameter values. Pattern formation in *Dictyostelium discoideum* pro-

vides the most well-studied case of this type of model. Although the model described in this section is based on only three equations, the excitable subsystem of the model arises from a much larger model which can be simplified by using the fact that there are a number of different timescales involved. The recent work by Weijer and coworkers has gone a long way in explaining a number of patterning phenomena that occur in *Dictyostelium discoideum* by including ideas from chemotaxis, excitable media and computational fluid dynamics (see Vasiev and Weijer, 2000, and references therein). Such single-cell systems, which are simpler to manipulate than embryos, may be important in providing crucial insights to some of the workings of more complicated multicellular organisms, and are therefore attracting more and more attention. For example, there is now a great deal of literature on the modelling of bacterial patterns (see Ben-Jacob *et al.*, 2000, and references therein).

All the above models are based on considering pattern formation at a macroscopic level. There is now an enormous amount known at the molecular level about pattern formation. One of the main future challenges is to develop models that can integrate the molecular and cellular levels.

3 Models for wound healing

Wound healing is an enormously complicated phenomenon involving different processes interacting on different spatio-temporal timescales (see, for example, the books by Clark and Henson, 1988, Asmussen and Söllner, 1993) and the method of healing varies depending on whether the wound is a surface wound (epidermal) or a deep wound (dermal), and on whether it is in the adult or the embryo. In this section we focus on a model for epithelial wound healing and one for dermal wound healing, and show how the ideas of modelling used in the previous section can be applied.

3.1 Corneal Wound Healing

Cell migration and proliferation are central to the healing of wounds in the corneal epithelium and biological evidence suggests that both processes are regulated by a protein called epidermal growth factor (EGF). The source of EGF is an area of controversy and the model of Dale *et al.* (1994) sets out to investigate the possibility that the exposed underlying tissue within the wound acts as an additional source to the overlying tear film layer.

Here, we summarise the model of Dale *et al.* (1994) and refer the reader to the original and references therein for full biological and modelling details. The model is a pair of reaction-diffusion equations for the cell density $n(\mathbf{x},t)$

and EGF concentration $c(\mathbf{x},t)$ at position $\mathbf{x}$ and time t and takes the form (suitably nondimensionalised)

$$\frac{\partial n}{\partial t} = \overbrace{\nabla\cdot(D_n(c)\nabla n)}^{\text{Cell Migration}} + \overbrace{s(c)n(2-n)}^{\text{Mitotic Generation}} - \overbrace{n}^{\text{Natural Loss}} \tag{24}$$

$$\frac{\partial c}{\partial t} = \underbrace{D_c\nabla^2 c}_{\text{Diffusion}} + \underbrace{f(n)}_{\text{Production by Cells}} - \underbrace{\frac{\mu n c}{(\hat{c}+c)} - \delta c}_{\text{Decay of Active EGF}} \tag{25}$$

where $D_n(c) = \alpha c+\beta$, and D_c, μ, δ, α , β and $\hat{c}$ are all positive constants. The model assumes that the cell diffusion coefficient is increased by EGF and $s(c)$ is an increasing function of c to account for the EGF-enhanced cell mitotis rate. The function $f(n)$ is taken to be of the form $f(n) = A + B(n)$, where

$$B(n) = \begin{cases} \sigma & \text{if } n < 0.2 \\ \sigma(2-5n) & \text{if } 0.2 \le n \le 0.4 \\ 0 & \text{if } n > 0.4 \end{cases}$$

and A and σ are positive constants. The A accounts for the constant source of EGF due to the tear film, while the function $B(n)$ is chosen to model EGF production due to wounding. The authors show that the detailed form of this function is not important to the behaviour of the model.

Using parameter values derived from the biological literature, this model system is solved on a one-dimensional domain (a realistic approximation for the case of surface slash wounds, where cell fronts move in from either side of the slash to close the wound) to investigate the behaviour of travelling wave solutions which move from a region where the cell density and EGF concentration are at their unwounded levels, $n = c = 1$ (as $x \to -\infty$), into a region of no cell density, $n = 0$, with the EGF concentration at its wounded level, $c = f(0)/\delta$ (as $x \to +\infty$).

An important conclusion from this work is that a realistic speed of healing is only attained if the function $B(n)$ is included (Figure 5). Hence the conclusion is that for the wound healing scenario envisaged by this model, biologically realistic healing times can only be achieved by assuming that the tear source of EGF is supplemented by EGF production in the wounded tissue.

For biologically realistic parameter values an analytical approximation to the minimum wavespeed can derived as $\sqrt{8\beta s(\frac{A+\sigma}{\delta})}$. An important biological implication of this result is that the rate of healing of corneal epithelial wounds can be increased by increasing the cell diffusion coefficient or the secretion rate of EGF. However, increasing the chemical diffusion coefficient does not have a

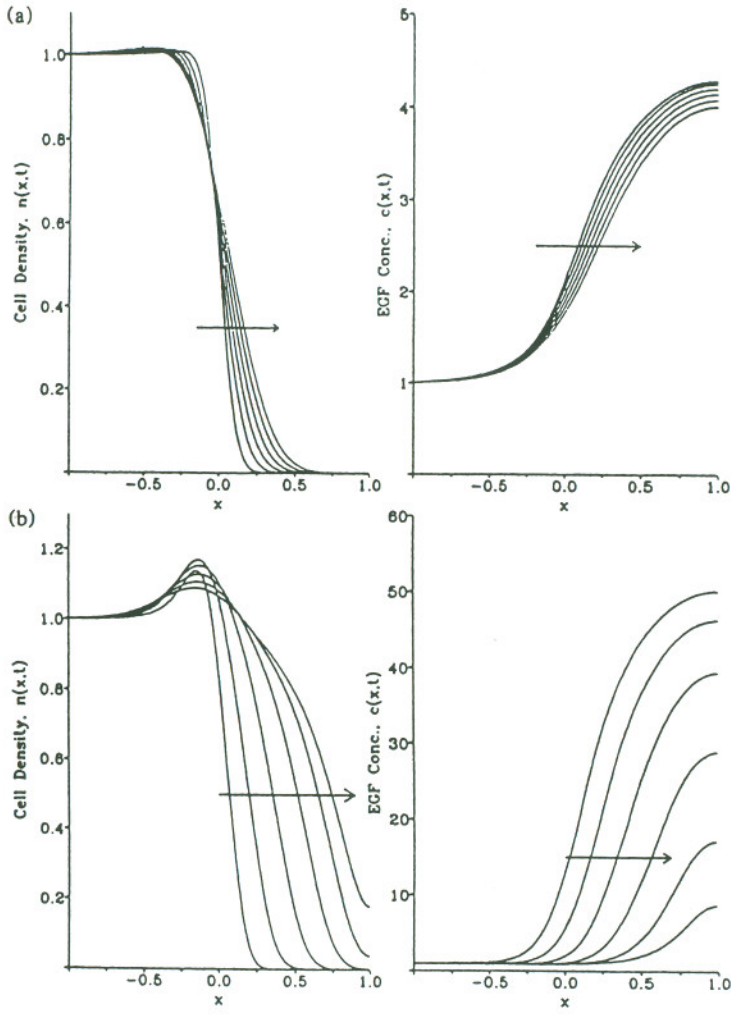

Figure 5. Numerical solution for the corneal wound healing model showing cell density and EGF concentration profiles as functions of space at equal time intervals. (a) The tear film is the only source of EGF, that is, $f(n) = A$. (b) An additional source of EGF is included, that is, $f(n) = A + B(n)$. Note that in (b) healing occurs much more rapidly. (Reproduced with permission from Dale *et al.*, 1994).

significant effect. The model can also be used to make experimentally testable predictions on how the speed of healing will change as the result of topical application of EGF.

3.2 Dermal healing

A crucial aspect of wound healing concerns the mechanical interaction of cells with their external environment. Cells deform and remodel the extracellular matrix on which they move and ECM materials, in turn, affect cellular properties and cell orientation. Using the mechanochemical model framework (see Murray, 1993, for review, and Murray *et al.*, 1988, Murray and Tranquillo, 1992) Olsen *et al.* (1995) developed a mechanochemical model for dermal wound healing. We refer the reader to the original paper for full details, including experimental justification for each term within the model. The model consists of two cell types – fibroblasts and myofibroblasts, densities, n and m, respectively; a generic growth factor, concentration c, and ECM, density ρ. These quantities obey the general conservation equation

$$\frac{\partial Q}{\partial t} = \nabla \cdot \mathbf{J_Q} + f_Q, \tag{26}$$

where Q is the quantity in question, the first term on the right-hand side models motion with flux $\mathbf{J_Q}$, and the second term models production and degradation. To complete the model, a force balance equation is needed to account for the mechanical interaction of the cells with the ECM.

For simplicity, we present here the one-dimensional version of the model, where x is space and t is time. The fibroblast cell equation takes the form:

$$\frac{\partial n}{\partial t} = D_n \frac{\partial^2 n}{\partial x^2} - \frac{\partial}{\partial x}[\chi(c,n)\frac{\partial c}{\partial n} + n\frac{\partial u}{\partial t}] + R(c)n(1 - \frac{n}{K}) - \frac{k_1 cn}{C_k + c} + k_2 m - d_n n. \tag{27}$$

Implicit in these equations is the assumption that there are three main factors contributing to cell flux: random diffusion, with constant diffusion coefficient, D_n; chemotaxis with chemotactic sensitivity $\chi(c,n)$, and advection in response to the displacement, $u(x,t)$, of the ECM. The four remaining terms on the right-hand side model cell kinetics and include logistic cell growth with linear rate enhanced by growth factor, fibroblast conversion to myofibroblast phenotype mediated by growth factor, conversion from myofibroblast back to fibroblast cell type, and cell death.

The myofibroblast equation takes the form

$$\frac{\partial m}{\partial t} = \frac{\partial}{\partial x}[-m\frac{\partial u}{\partial t}] + \epsilon_r R(c)m(1 - \frac{m}{K}) + \frac{k_1 cn}{C_k + c} - k_2 m - d_m m. \tag{28}$$

Here, it is assumed that the dominant contribution to myofibroblast flux is advection, and that mitosis takes the same form as that for fibroblasts, modulated by a constant scale factor ϵ_r.

The growth factor satisfies the equation

$$\frac{\partial c}{\partial t} = D_c \frac{\partial^2 c}{\partial x^2} + \frac{\partial}{\partial x}[-c\frac{\partial u}{\partial t}] + S(n, m, c) - d_c c. \tag{29}$$

Implicit in this equation is the assumption that the dominant contributions to growth factor flux are random diffusion, with constant diffusion coefficient D_c, and advection. The remaining terms on the right-hand side model biosynthesis and degradation.

The ECM moves primarily by advection and satisfies the equation

$$\frac{\partial \rho}{\partial t} = \frac{\partial}{\partial x}[-\rho\frac{\partial u}{\partial t}] + B(n, m.c, \rho), \tag{30}$$

where $B(n, m, c, \rho)$ represents ECM biosynthesis and degradation.

Finally, modelling the ECM as a linear, isotropic, viscoelastic material, the displacement u satisfies the force balance equation

$$\mu\frac{\partial^3 u}{\partial x^2 \partial t} + E\frac{\partial^2 u}{\partial x^2} + \frac{\partial \tau(n, \rho)}{\partial x} = F(\rho, u), \tag{31}$$

where the first two terms on the left-hand side model viscous and elastic forces, respectively, and the third term models cell traction forces. These forces are balanced by the body forces $F(\rho, u)$. Note that this is very much a simplification as a more realistic model should include anisotropy and plasticity.

The above five equations, with appropriate initial and boundary conditions (see below) constitute the mechanochemical model framework. Solving these equations in one spatial dimension is an approximation to "slash" wounds. Numerical simulations show that these equations admit solutions in which a travelling front of cell density moves into the wound, causing it to heal. Using biologically realistic forms for the functions $\chi(c, n), R(c), S(n, m, c), B(n, m.c, \rho), \tau(n, \rho), F(\rho, u)$, and estimates derived from experimental data for the parameters $D_n, D_c, K, k_1, k_2, C_k, d_n, d_m, d_c, \epsilon_r, \mu$ and E, it can be shown that this model exhibits solutions for the decay of growth factor and rate of wound closure that closely agree with experimental results (see Olsen *et al.*, 1995, for full details).

This model can be used to investigate abnormal wound healing. The full model is very complicated so simpler caricatures are considered. To investigate the potential of the above model framework to exhibit spatially-varying contracted steady states, corresponding to fibrocontractive diseases, Olsen *et al.* 1998, considered a simpler version of the model which focusses only on the mechanical aspects of the interaction. The non-dimensionalised version of this caricature model takes the form

$$\frac{\partial n}{\partial t} = D_n \frac{\partial^2 n}{\partial x^2} + \frac{\partial}{\partial x}[-n\frac{\partial u}{\partial t}] + n(1-n) \tag{32}$$

$$\frac{\partial \rho}{\partial t} = \frac{\partial}{\partial x}[-\rho\frac{\partial u}{\partial t}] \tag{33}$$

$$\mu\frac{\partial^3 u}{\partial x^2 \partial t} + E\frac{\partial^2 u}{\partial x^2} + \frac{\partial \tau(n, \rho)}{\partial x} = F(\rho, u). \tag{34}$$

This caricature considers only the fibroblast cell type and assumes a simple form for logistic growth. It also assumes that there is negligible synthesis and degradation of ECM on the timescale of wound closure. This is a reasonable assumption to make in the stages prior to tissue remodelling during the process of wound healing.

By defining the initial wound space as $-1 \leq x \leq 1$ and using symmetry at $x = 0$ (the wound centre), we may restrict attention to the semi-infinite domain $0 \leq x < \infty$. The boundary conditions are thus

$$\frac{\partial n}{\partial x}(0, t) = \frac{\partial \rho}{\partial x}(0, t) = u(0, t) = 0 \quad \text{and} \quad n(\infty, t) = \rho(\infty, t) = 1, \quad u(\infty, t) = 0.$$

The initial conditions are

$$n(x, 0) = H(x-1), \quad \rho(x, 0) = \rho_i + (1-\rho_i)\, H(x-1), \quad u(x, 0) = 0,$$

where the initial ECM density ρ_i inside the wound is due to the early, provisional wound matrix which is low in collagen and satisfies $0 < \rho_i < 1$, and $H(\cdot)$ is the Heaviside step function.

Consider now the healed steady state, $n = 1$. Linearising the matrix equation about the initial profile, we have

$$\rho \approx \begin{cases} \rho_i\,(1 - \partial u/\partial x)\,, & 0 \leq x < 1 \\ 1 - \partial u/\partial x, & x > 1 \end{cases} \tag{35}$$

as suggested by the small-strain restriction (since the convective flux should be small). Substituting this into the steady state equation for u results in a second order ordinary differential equation for u which can be written in the (rescaled) form

$$u' = v \tag{36}$$

$$v' = \begin{cases} \dfrac{s\rho_i u(1-v)}{1-\rho_i \mathcal{T}[\rho_i(1-v)]}, & 0 \le x < 1 \\ \dfrac{su(1-v)}{1-\mathcal{T}(1-v)}, & x > 1 \end{cases} \tag{37}$$

where $\mathcal{T}(\rho) \equiv \left.\frac{\partial \tau(n,\rho)}{\partial \rho}\right|_{n=1}$, and u satisfies the boundary conditions $u(0) = u(\infty) = 0$. Here it is assumed that the body force, $F(\rho, u)$, is due to external tethering to the basement membrane and have modelled it by a linear spring, that is, $F(\rho, u) = su\rho$, where s is a constant.

Standard phase plane analysis of (36)–(37) shows that for $x > 1$, the origin is a saddle (centre) iff $\mathcal{T}(1) < 1 (> 1)$. Linear stability analysis of the caricature model (32)–(34) shows that a necessary (but not sufficient) condition for the healed steady state to be stable is $\mathcal{T}(1) < 1$ (see Olsen *et al.*, 1998). As this must be the case for the model to be realistic biologically, we have that the origin of the ordinary differential equation system (36)–(37) is a saddle, and the boundary condition $u(\infty) = 0$ implies that the solution must converge towards the origin along the stable manifold as x tends to ∞. By tracing backwards in x from infinity along the stable manifold, the solution reaches a point in the (u, u')-phase plane corresponding to $x = 1$ where $u = u_1$, say. This must match the solution for $0 \le x < 1$.

Now, at the wound centre, $u(0) = 0$, but $v(0)$ is unspecified and is determined by matching to the "outer" solution at $x = 1$. For $0 \le x < 1$, it can be shown that the origin can either be a saddle or a centre, depending on the form of the function $\tau(n, \rho)$ and the values of the other parameters. If the origin is a saddle point, then the solution in $0 \le x < 1$ will be either monotonic increasing with increasing gradient or monotonic decreasing with decreasing gradient. If the origin is a centre, then the solution in $0 \le x < 1$ may be oscillatory. Figure 6 illustrates the qualitative construction of such a solution and Figure 7 illustrates various possible forms of steady state solutions based on this construction. Modelling the traction term, $\tau(n, \rho)$, by $\tau(n, \rho) = \tau_0 n\rho/(T^2 + \rho^2)$, where τ_0 and T are constant parameters, to account for the fact that traction forces depend on adhesion between cell surface receptors and binding sites on collagen fibres, but the ability of a cell to extend and retract protrusions within a collagen substrate is inhibited at relatively high collagen densities, steady states for (32)–(34) of the form illustrated in Figure 7(a)–(e) can be found by numerical simulation.

Hence, this caricature model enables us to more fully understand the properties of the full model and shows clearly that the model can exhibit spatially-varying contracted steady states, and is thus consistent with clinical observations on normal healing. For full details, see Olsen *et al.* 1998.

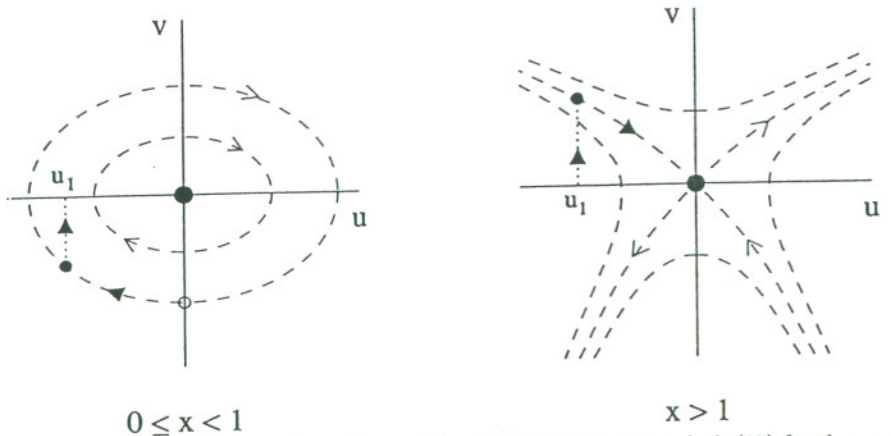

Figure 6. Qualitative illustration of a possible solution trajectory to (36)–(37) for the case in which the origin is a centre for $0 \le x < 1$ and a saddle point for $x > 1$ with $u(x) \to 0$ from below as $x \to \infty$. See also Figure 7(b). Dashed curves denote phase trajectories, with the contracted solution curve highlighted by solid arrows. See text for details. (Reproduced with permission from Olsen *et al.*, 1997).

We now consider the application of the model to fibroproliferative wound healing disorders. These disorders are characterised by the generation of abnormally large amounts of tissue during the healing process, leading to, for example, keloid scarring. Numerical simulations of the full model show that it can exhibit solutions in which an excess of cells is observed, corresponding to a pathological state. To understand this more fully, a caricature model of the full system is, again, investigated. In this case, however, we focus purely on the chemical aspects of the mechanochemical framework by considering the cell-chemical sub-model

$$\frac{\partial n}{\partial t} = D_n \frac{\partial^2 n}{\partial x^2} - \frac{\partial}{\partial x}\left[\chi(c,n)\frac{\partial c}{\partial n}\right] + \sigma\left[1 + \frac{Pc}{Q+c}\right] n(1 - \frac{n}{K}) - d_n n \tag{38}$$

$$\frac{\partial c}{\partial t} = D_c \frac{\partial^2 c}{\partial x^2} + \frac{\kappa_c n c}{\gamma + c} - d_c c, \tag{39}$$

where $\chi(c, n) = \alpha/(\beta + c)^2$, and $\alpha, \beta, P, Q, \kappa_c$ and γ are positive constants (see Olsen *et al.*, 1996 for full details).

This caricature model has two uniform steady states, $(n, c) = (0, 0), (K, 0)$ corresponding, respectively, to the trivial, or non-healing, state, and the nor-

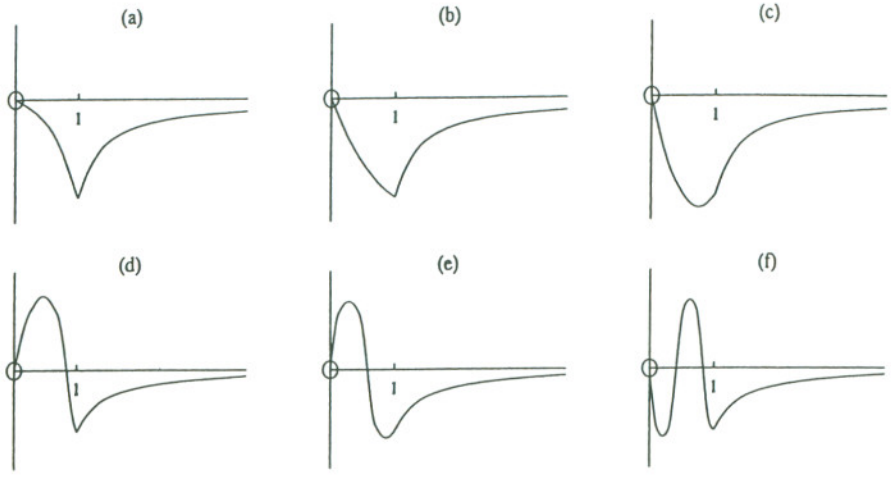

Figure 7. Possible qualitative forms of the solution $u(x)$ of the boundary value problem (36)–(37), representing contracted tissue displacement profiles. The point $(u, u') = (0, 0)$ must be a saddle point for $x > 1$ in the (u, u')-phase plane, with u increasing to zero and u' decreasing to zero monotonically along the stable manifold in the top-left quadrant as $x \to \infty$. For $0 \leq x < 1$, the origin may be either a saddle point, in which case the profiles for u and u' are monotonic decreasing as shown in (a), or a centre, in which case u and u' oscillate about the origin as shown in (b–f); within this region, any number of oscillations is possible—for example, (f) is equivalent to (b) modulo one period. Note that the above steady-state profiles but with reversed signs of u and u' are also admissible solutions of (36)–(37), representing expanded tissue displacement profiles since $u(1)$ would be positive. Recall that $x = 1$ is the initial wound boundary. (Reproduced with permission from Olsen *et al.*, 1997).

mal dermal state. For appropriate parameter values, two other steady states exist which have both n and c non-zero, with $n > K$. These are the pathological, or diseased, steady states. Results from bifurcation analysis of (38)–(39), in the absence of diffusion, show that for a critical value, κ_c^1, of κ_c (which can be found in terms of the other parameters) the dermal steady state remains locally stable but loses global stability as the pathological steady states appear. At $\kappa_c = \kappa_c^2$, the dermal steady state loses stability and the pathological state with higher cell density level becomes globally stable.

A travelling wave analysis of the model shows that trajectories from the dermal state to the pathological state are possible and a minimum wavespeed

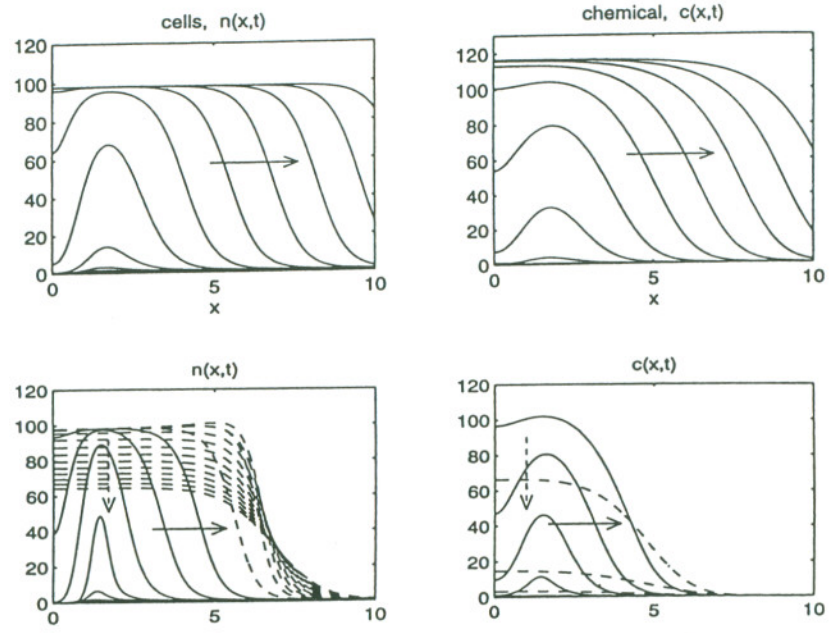

Figure 8. Numerical simulations of (38)–(39) showing progression to pathological steady state (a), and cessation and regression for the case where κ_c is reduced to zero after a certain time (b). (Reproduced with permission from Olsen *et al.*, 1997).

can be determined. Numerical simulations of the system show that such travelling waves do exist, but that reducing κ_c can cause the waves to stop and to regress (see Figure 8). This suggests that the reduction of the rate at which cells secrete growth factor can cause the disease to regress back to the normal dermal state. More detailed analysis of this model determines analytically how the bifurcation values of κ_c depend on the other parameters in the model. In particular, the model exhibits hysteresis and therefore, counter-intuitively, κ_c must be reduced considerably in order to progress from the diseased state to a healed state. This provides a clinically-testable method to help reduce this type of fibroproliferative disorder.

It should be noted that although the above studies were carried out for simplified versions of the full mechanochemical model, the results do indeed

hold for the full model.

3.3 Discussion

The above models have been presented to illustrate how continuum type models can be used to address problems in normal and abnormal wound healing. The model for corneal wound healing has recently been extended to be more biologically realistic by including more than one cell type. The resultant model is a system of coupled integro-partial differential equations which exhibits mitotic profiles that are more biologically realistic than those observed in the original model (Gaffney *et al.*, 1999).

The mechanochemical modelling framework can be extended to include cell alignment and matrix orientation, the latter is thought to play a crucial role in determining the severity of scar tissue formation (Olsen *et al.*, 1999, Dallon *et al.*, 1999). This particular modelling framework assumes that the extracellular matrix is a linear viscoelastic material. However, it is clearly more complicated than that and a more realistic model, considering the ECM as a viscoelastic-plastic material has recently been proposed (Tracqui *et al.*, 1995).

None of the above models investigate angiogenesis, the process by which new blood vessels form. This is of great interest also in tumour formation, where after reaching a certain size, limited by the availability of nutrients via simple diffusion, a tumour can only grow further by establishing its own blood supply via the release of so-called tumour angiogenesis factor. This is what allows the tumour to grow and undergo metastasis, causing the growth of secondary tumours which are usually fatal. For the mathematical modelling of angiogenesis in wound healing, the reader is referred to the paper by Byrne and Chaplain (1995), while the papers by Pettet *et al.* (1996) and Olsen *et al.* (1997) address wound healing angiogenesis.

4 Conclusions

In this paper I have considered the problems of spatial pattern formation in biology and of wound healing by illustrating a few applications. These seemingly unrelated processes share the common underlying theme of cell response to, and interaction with, signalling cues. The models are conceptually simple and closely related, yet exhibit a bewildering array of behaviours, from spiral waves, spots and stripes, with application in pattern formation, to travelling waves of invasion in wound healing.

The material in Sections 2 and 3 has illustrated how mathematical models

can be used to gain important insights to the underlying mechanisms responsible for spatio-temporal pattern formation in biology and normal/abnormal wound healing and to make experimentally testable predictions. It is clear that even these so-called simple models pose challenging problems to the mathematician. Many of the results presented here were obtained from numerical simulation. An important future aim will be to make some of these results mathematically realistic.

Over the past decade there have been huge advances in molecular biology. A key problem for the next decade will be to combine this knowledge with research in cellular biology to gain a fuller understanding of the systems being studied. Important scientific advances in this area will only be made by a truly interdisciplinary approach and it is clear that mathematical modelling and numerical computation will have important roles to play in this endeavour. It is also clear that biology and medicine will continue to be a source of novel, difficult and challenging problems for mathematicians and numerical analysts.

References

1. J.L. Aragón, C. Varea, R.A. Barrio and P.K. Maini, Spatial patterning in modified Turing systems: Application to pigmentation patterns on marine fish, *FORMA*, **13**, 213–221 (1998)
2. P.D. Asmussen and B. Söllner: Wound care: Principles of wound healing. *Beierdorf Medical Bibliothek* (1993)
3. J.B.L. Bard, A model for generating aspects of zebra and other mammalian coat patterns, *J. theor. Biol.*, **93**, 363–385 (1981)
4. J.B.L. Bard and I. Lauder, How well does Turing's theory of morphogenesis work? *J. theor. Biol.*, **45**, 501–531 (1974)
5. D.L. Benson, P.K. Maini and J.A. Sherratt, Unravelling the Turing bifurcation using spatially varying diffusion coefficients, *J. Math. Biol.*, **37**, 381–417 (1998)
6. E. Ben-Jacob, I. Cohen, I. Golding and Y. Kozlovsky, Modeling branching and chiral colonial patterning of lubricating bacteria, In: *Proceedings of IMA Workshop on Pattern Formation*, H.G. Othmer and P.K. Maini, (eds) to appear (2000).
7. N.F. Britton, *Reaction-Diffusion Equations and Their Applications to Biology*, Academic Press, London (1986)
8. F. Brümmer, G. Zempel, P. Buhle, J.-C. Stein and D.F. Hulser, Retinoic acid modulates gap junction permeability: A comparative study of dye spreading and ionic coupling in cultured cells, *Exp. Cell. Res.*, **196**, 158–163 (1991)

9. H.M. Byrne and M.A.J. Chaplain, Mathematical models for tumour angiogenesis: numerical simulations and nonlinear wave solutions, *Bull. Math. Biol.*, **57**, 416–486 (1995)
10. H.M. Byrne and M.A.J. Chaplain, On the importance of constitutive equations in mechanochemical models of pattern formation, *Appl. Math. Lett.*, **9**, 85–90 (1996)
11. V. Castets, E. Dulos, J. Boissonade and P. De Kepper, Experimental evidence of a sustained Turing-type equilibrium chemical pattern, *Phys. Rev. Lett.*, **64**(3), 2953–2956 (1990)
12. R.A.F. Clark and P.M. Henson (eds.), *The Molecular and Cellular Biology of Wound Repair*, Plenum Press, New York (1988)
13. G. Cocho, R. Pérez-Pascual and J.L. Rius, Discrete systems, cell-cell interactions and color pattern of animals. I. Conflicting dynamics and pattern formation, *J. theor. Biol.*, **125**, 419–435 (1987a)
14. G. Cocho, R. Pérez-Pascual, J.L. Rius and F. Soto, Discrete systems, cell-cell interactions and color pattern of animals. I. Clonal theory and cellular automata, *J. theor. Biol.*, **125**, 437–447 (1987b)
15. E.J. Crampin, E.A. Gaffney and P.K. Maini, Reaction and Diffusion on Growing Domains: Scenarios for Robust Pattern Formation, *Bull. Math. Biol.*, **61**, 1093–1120 (1999)
16. P.D. Dale, P.K. Maini and J.A. Sherratt, Mathematical modelling of corneal epithelium wound healing, *Math. Biosciences*, **124**, 127–147 (1994)
17. J. Dallon, J. Sherratt and P.K. Maini, Mathematical modelling of extracellular matrix dynamics using discrete cells: Fiber orientation and tissue regeneration, *J. theor. Biol.*, **199**, 449–471 (1999)
18. A. Davidson, M.A.R. Koehl, R. Keller and G.F. Oster, How do sea urchins invaginate? Using biomechanics to distinguish between mechanisms of primary invagination, *Dev.*, **121**, 2005–2018 (1995).
19. P. De Kepper, V. Castets, E. Dulos and J. Boissonade, Turing-type chemical patterns in the chlorite-iodide-malonic acid reaction, *Physica D*, **49**, 161–169 (1991)
20. R. Dillon, P.K. Maini and H.G. Othmer, Pattern formation in generalised Turing systems: I. Steady-state patterns in systems with mixed boundary conditions, *J. Math. Biol.*, **32**, 345–393 (1994)
21. L. Edelstein-Keshet, *Mathematical Models in Biology*, New York, Random House (1988)
22. B. Ermentrout, Stripes or spots? Nonlinear effects in bifurcation of reaction-diffusion equations on the square, *Proc. Roy. Soc. Lond.*, **A434**, 413–417 (1991)

23. B. Ermentrout, J. Campbell and G. Oster, A model for shell patterns based on neural activity, *The Veliger*, **28**, 369-338 (1986)
24. P. Fife, *Mathematical Aspects of Reacting and Diffusing Systems, Lect. Notes in Biomath.*, **28**, Springer-Verlag, Berlin, Heidelberg, New York (1979)
25. E.A. Gaffney, P.K. Maini, J.A. Sherratt and S. Tuft, The mathematical modelling of cell kinetics in corneal epithelial wound healing, *J. theor. Biol.*, **197**, 15–40 (1999)
26. A. Gierer and H. Meinhardt, A theory of biological pattern formation, *Kybernetik*, **12**, 30–39 (1972)
27. P. Grindrod, *The Theory of Applications of Reaction-Diffusion Equations: Pattern and Waves*, Oxford University Press (1996)
28. J.D. Gross, M.J. Peacey and D.J. Trevan, Signal emission and signal propagation during early aggregation in *Dictyostelium discoideum*, *J. Cell Sci.*, **22**, 645–656 (1976)
29. T. Höfer, P.K. Maini, J.A. Sherratt, M.A.J. Chaplain, P. Chauvet, D. Metevier, P.C. Montes and J.D. Murray, A resolution of the chemotactic wave paradox, *Appl. Math. Lett.*, **7**, 1–5 (1994)
30. T. Höfer, J.A. Sherratt and P.K. Maini, *Dictyostelium discoideum*: cellular self-organization in an excitable biological medium, *Proc. Roy. Soc. Lond. B* **259**, 249–257 (1995a)
31. T. Höfer, J.A. Sherratt and P.K. Maini, Cellular pattern formation during *Dictyostelium* aggregation, *Physica D*, **85**, 425–444 (1995b)
32. D.M. Holloway and L.G. Harrison, Algal morphogenesis: modelling interspecific variation in *Micrasterias* with reaction-diffusion patterned catalysis of cell surface growth, *Phil. Trans. R. Soc. Lond.*, **B354**, 417–433 (1999)
33. B.R. Johnson and S.K. Scott, New approaches to chemical patterns, *Chem. Soc. Rev.*, 265–273 (1996)
34. E.F. Keller and L.A. Segel, Travelling bands of bacteria: a theoretical analysis, *J. theor. Biol.*, **30**, 235–248 (1971)
35. S. Kondo and R. Asai, A reaction-diffusion wave on the skin of the marine angelfish *Pomacanthus*, *Nature*, **376**, 765–768
36. P.M. Kulesa, G.C. Cruywagen, S.R. Lubkin, P.K. Maini, J. Sneyd, M.W.J. Ferguson and J.D. Murray, On a model mechanism for the spatial patterning of teeth primordia in the Alligator, *J. theor. Biol.*, 180, 287–296 (1996)
37. L. Landau and E. Lifshitz, *Theory of Elasticity*, Pergamon Press, New York (1970)
38. I. Lengyel and I.R. Epstein, Modeling of Turing structures in the chlorite-

iodide-malonic acid-starch reaction system, *Science,* **251,** 650–652 (1991)
39. P.K. Maini and M. Solursh, Cellular mechanisms of pattern formation in the developing limb, *Int. Rev. Cytology,* **129,** 91–133 (1991)
40. P.K. Maini, D.L. Benson and J.A. Sherratt, Pattern formation in reaction diffusion models with spatially inhomogeneous diffusion coefficients, *IMA J.Math.Appl.Med. & Biol.*, **9,** 197–213 (1992)
41. P.K. Maini, M.R. Myerscough, K.H. Winters and J.D.Murray, Bifurcating spatially heterogeneous solutions in a chemotaxis model for biological pattern formation, *Bull. Math. Biol.*, **53,** 701–719 (1991)
42. J.L. Martiel and A. Goldbeter, A model based on receptor desensitization for cyclic AMP signaling in *Dictyostelium* cells, *Biophys. J.*, **52,** 807–828 (1987)
43. H. Meinhardt, *Models of Biological Pattern Formation*, Academic Press (1982)
44. H. Meinhardt, *The Algorithmic Beauty of Sea Shells*, Springer-Verlag (1995)
45. J.D. Murray, A pre-pattern formation mechanism for animal coat markings, *J. theor. Biol.*, **88,** 161–199 (1981)
46. J.D. Murray, Parameter space for Turing instability in reaction-diffusion mechanisms: a comparison of models, J. theor. Biol., **98,** 143–163 (1982)
47. J.D. Murray *Mathematical Biology*, Springer-Verlag (1993)
48. J.D. Murray, D.C. Deeming, D.C. and M.W.J. Ferguson, Size dependent pigmentation pattern formation in embryos of Alligator mississippiensis: time of initiation of pattern generation mechanism, *Proc. Roy. Soc. Lond.*, **B 239,** 279–293 (1990)
49. J.D. Murray, P.K. Maini and R.T. Tranquillo, Mechanochemical models for generating biological pattern and form in development, *Physics Reports,* **171,** 59–84 (1988)
50. J.D. Murray and M.R. Myerscough, Pigmentation pattern formation on snakes, *J. theor. Biol.*, **149,** 339–360 (1991)
51. J.D. Murray and R.T. Tranquillo, Continuum of fibroblast-driven wound contraction: inflammation-mediation, *J. theor. Biol.*, **158,** 135–172 (1992)
52. B.N. Nagorcka, Wavelike isomorphic prepatterns in development, *J. theor. Biol.*, **137,** 127–162 (1989)
53. B.N. Nagorcka, V.S. Manoranjan and J.D. Murray, Complex spatial patterns from tissue interactions — an illustrative model, *J. theor. Biol.*, **128,** 359–374 (1987)
54. G.A. Ngwa and P.K. Maini, Spatio-temporal patterns in a mechanical model for mesenchymal morphogenesis, *J. Math. Biol.*, **33,** 489–520 (1995)

55. H.F. Nijhout, A comprehensive model for colour pattern formation in butterflies, *Proc. R. Soc. Lond. B* **239,** 81–113 (1990)
56. G.M. Odell, G. Oster, P. Alberch and B. Burnside, The mechanical basis of morphogenesis. I. Epithelial folding and invagination, *Devl. Biol.*, **85,** 446–462 (1981)
57. L. Olsen, J.A. Sherratt and P.K. Maini, A mechanochemical model for adult dermal wound contraction and the permanence of the contracted tissue displacement profile, *J. theor. Biol.*, **177,** 113–128 (1995)
58. L. Olsen, J.A. Sherratt and P.K. Maini, A mechanochemical model for adult dermal wound contraction: On the permanence of the contracted tissue displacement profile, *J. theor. Biol.*, **177,** 113–128 (1995)
59. L. Olsen, J.A. Sherratt and P.K. Maini, A mathematical model for fibroproliferative wound healing disorders, *Bull. Math. Biol.*, **58,** 787–808 (1996)
60. L. Olsen, P.K. Maini and J.A. Sherratt, Spatially varying equilibria of mechanical models: application to dermal wound contraction, *Math. Biosciences*, **147**, 113–129 (1998)
61. L. Olsen, J.A. Sherratt, P.K. Maini and F. Arnold, A mathematical model for the capillary endothelial cell-extracellular matrix interactions in wound-healing angiogenesis, *IMA J.Math.Appl.Med. & Biol.*, **14(4),** 261–281 (1997)
62. L. Olsen, P.K. Maini, J.A. Sherratt and J. Dallon, Mathematical modelling of anisotropy in fibrous connective tissue, *Math. Biosciences,* **158,** 145–170 (1999)
63. G.F. Oster and J.D. Murray, Pattern formation models and development, *Zool.*, **251,** 186–202 (1989)
64. G.F. Oster, J.D. Murray and A.K. Harris, Mechanical aspects of mesenchymal morphogenesis, *J. Embryol.exp. Morph.*, **78,** 83–125 (1983)
65. H.G. Othmer and A. Stevens, Aggregation, blowup, and collapse: The ABC's of taxis in reinforced random walks, *SIAM J. Appl. Math.*, **57,** 1044–1081 (1997)
66. A.V. Panfilov and A.V. Holden (eds), Computational Biology of the Heart, Chichester, John Wiley & Sons (1997)
67. K.J. Painter, P.K. Maini and H.G. Othmer, A chemotactic model for the advance and retreat of the primitive streak in avian development, *Bull. Math. Biol.* (to appear) (1999a)
68. K.J. Painter, P.K. Maini and H.G. Othmer, Stripe formation in juvenile *Pomacanthus* explained by a generalised Turing mechanism with chemotaxis, *PNAS*, **96**, 5549–5554 (1999b)

69. A.S. Perelson, P.K. Maini, J.D. Murray, J.M. Hyman and G.F. Oster, Nonlinear pattern selection in a mechanical model for morphogenesis, *J. Math. Biol.*, **24,** 525–541 (1986)
70. G. Pettet, M.A.J. Chaplain, D.L.S. McElwain and H.M. Byrne, On the role of angiogenesis in wound healing, *Proc. Roy. Soc. Lond.*, **B263,** 1487–1493 (1996)
71. J. Schnakenberg, Simple chemical reaction systems with limit cycle behaviour, *J. theor. Biol.*, **81,** 389–400 (1979)
72. L.A. Segel, *Modelling Dynamic Phenomena in Molecular and Cellular Biology*, Cambridge, Cambridge University Press (1984)
73. D.R. Soll, D. Wessels and A. Sylwester, The motile behavior of amoebae in the aggregation wave in *Dictyostelium discoideum*, In: *Experimental and Theoretical Advances in Biological Pattern Formation*, H.G. Othmer, P.K. Maini and J.D. Murray, (eds.), Plenum Press, London, pp 325–328 (1993)
74. M.S. Steinberg, Does differential adhesion govern self-assembly processes in histogenesis? Equilibrium configurations and the emergence of a hierarchy among populations of embryonic cells, J. exp. Zool., **173,** 395–434 (1970)
75. D. Sulsky, S. Childress and J.K. Percus, A model of cell sorting, *J. theor. Biol.*, **106,** 275–301 (1984)
76. D. Thomas, Artifical enzyme membranes, transport, memory and oscillatory phenomena, in *Analysis and Control of Immobilized Enzyme Systems*, ed. D. Thomas and J.-P. Kernevez, Springer, Berlin, Heidelberg, New York, 115–150 (1975)
77. P. Tracqui, D.E. Woodward, G.C. Cruywagen, J. Cook and J.D. Murray, A mechanical model for fibroblast-driven wound healing, *J. Biol. Systems,* **3,** 1075–1085 (1995)
78. A.M. Turing, The chemical basis of morphogenesis, *Phil. Trans. Roy. Soc. Lond. B* **327**, 37–72 (1952)
79. J.J. Tyson and J.P. Keener, Singular perturbation theory of traveling waves in excitable media (a review), *Physica D,* **32,** 327–361 (1988)
80. B. Vasiev and C.J. Weijer, Modelling *Dictystelium Discoideum* morphogenesis, In: *Proceedings of IMA Workshop on Pattern Formation*, H.G. Othmer and P.K. Maini, (eds) to appear (2000).
81. M. Weliky, S. Minsuk, R. Keller and G.F. Oster, Notochord morphogenesis in *Xenopus laevis*: simulation of cell behaviour underlying tissue convergence and extension, *Dev.*, **113,** 1231–1244 (1991)
82. M. Weliky and G.F. Oster, The mechanical basis of cell rearrangement. I. Epithelial morphogenesis during *Fundulus* epiboly, *Dev.*, **109,** 373–386 (1990)
83. L. Wolpert, Positional information and the spatial pattern of cellular differentiation, *J. theor. Biol.*, **25,** 1–47 (1969)
84. L. Wolpert and A. Hornbruch, Double anterior chick limb buds and models for cartilage rudiment specification, *Development,* **109,** 961–966 (1990)